Acta Crystallographica Section B
Structural Science
ISSN 0108-7681

Two-dimensionally modulated structure of the rare-earth polysulfide GdS_{2-x} ($x = 0.18 \simeq 13/72$)

Rafael Tamazyan,[a]* Sander van Smaalen,[b] Inga Grigorevna Vasilyeva[c] and Heinrich Arnold[d]

[a]Molecular Structure Research Center, National Academy of Science, Republic of Armenia, [b]Laboratory of Crystallography, University of Bayreuth, 95440 Bayreuth, Germany, [c]Institute of Inorganic Chemistry, Siberian Branch, Russian Academy of Science, Novosibirsk, Russia, and [d]Institut für Kristallographie, RWTH Aachen, Germany

Correspondence e-mail: rafael@msrc.am

Received 9 May 2003
Accepted 6 October 2003

The crystal structure of GdS_{2-x} is determined by single-crystal X-ray diffraction as a 144-fold superstructure of the ZrSSi structure type. The superstructure is described as a two-dimensional, commensurately modulated structure with the superspace group $P4/n(\alpha\beta\frac{1}{2})(00)(ss)$ and with $\alpha = 1/4$ and $\beta = 1/3$. Structure refinements within the classical approach, employing the 144-fold supercell, fail because most of the superlattice reflections have zero intensities within the experimental resolution. Within the superspace approach the absent superlattice reflections are systematically classified as higher-order satellite reflections. Accordingly, the superspace approach has been used to refine the structure model comprising the basic structure positions and the amplitudes of the modulation functions of the three crystallographically independent atoms. The quality of fit to the diffraction data and the values of the refined parameters are independent of the assumption on the true symmetry (incommensurate or a $12 \times 12 \times 2$, *I*-centred superlattice with different symmetries). Arguments of structural plausibility then suggest that the true structure is a superstructure with space group $I\bar{4}$, corresponding to sections of superspace given by (t_1, t_2) equal to $[(4n-1)/48, (4m-3)/48]$ or $[(4n-3)/48, (4m-1)/48]$ (n and m are integers). Analysis of the structure, employing both superspace techniques (t plots) and the supercell structure model all show that the superstructure corresponds to an ordering of vacancies and an orientational ordering of S_2^{2-} dimers within the square layers of the S2 atoms.

1. Introduction

GdS_{2-x} belongs to the family of rare-earth (RE) polychalcogenides. These compounds have been studied because of their interesting physical properties, which can be tuned by changing the composition x. In particular, the charge-density wave (CDW) states have been predicted by band-structure calculations for some RE polychalcogenides (Lee & Foran, 1994, 1996; Stöwe, 2000). These calculations have shown that the physical properties of these compounds depend strongly on the details of their crystal structures. In the last few years the RE polychalcogenides containing the heavier chalcogen atoms Se and Te have been intensively investigated in Dresden (Fokwa *et al.*, 2002*a*,*b*; Fokwa, Doert & Böttcher, 2002; Wu *et al.*, 2002*a*,*b*; Dashjav, Doert *et al.*, 2000; Dashjav, Oeckler *et al.*, 2000), while the RE polychalcogenides with the lighter chalcogen atom S have been studied at the Institute of Inorganic Chemistry of the Siberian Branch of the Russian Academy of Sciences (Vasilyeva & Kurochkina, 1981; Vasilyeva, 1985; Podberezskaya *et al.*, 1998, 1999, 2001).

The crystal structures of RE polychalcogenides are based on the ZrSSi structure type (also known as the PbFCl structure type; Villars & Calvert, 1996). This structure type is built from the two-atom thick layers ReX, corresponding to a (100) slab of the NaCl structure type, alternating with planes of X atoms on a square lattice (Fig. 1). Accordingly, the chemical composition of the RE polychalcogenides can be written as [ReX][X]. Assuming the usual oxidation states Re^{3+} for the rare-earth atoms and X^{2-} for the isolated chalcogen atoms in the ReX layers, the X atoms in square layers must be present as oligomeric X_n^{n-} anions (Böttcher, 1988; Böttcher & Doert, 1998; Böttcher *et al.*, 2000). Different types of polyanions have been observed for RE chalcogenides with heavy chalcogen atoms (X = Se, Te; Wu *et al.*, 2002*a*,*b*; Dashjav, Doert *et al.*, 2000; Dashjav, Oeckler *et al.*, 2000), but only S_2^{2-} dimers have been observed for polysulfides (Tamazyan *et al.*, 1994; Podberezskaya *et al.*, 1998, 1999; Tamazyan *et al.*, 2000*a*,*b*).

In the nonstoichiometric X-deficient compounds ReX_{2-x} vacancies are concentrated in the square layers. The ordering of vacancies and the orientational ordering of polyanions give rise to a rich family of superstructures. Taking the charge balance into account, the chemical formula is now $[Re^{3+}X^{2-}][(X_2^{2-})_{\frac{1}{2}-x}(X^{2-})_x\square_x]$. Theoretical calculations show a strong dependence of the electronic band structures and possible CDW states on the lattice distortions and ordering processes in the square layers. They point out the importance of structural investigations of these compounds.

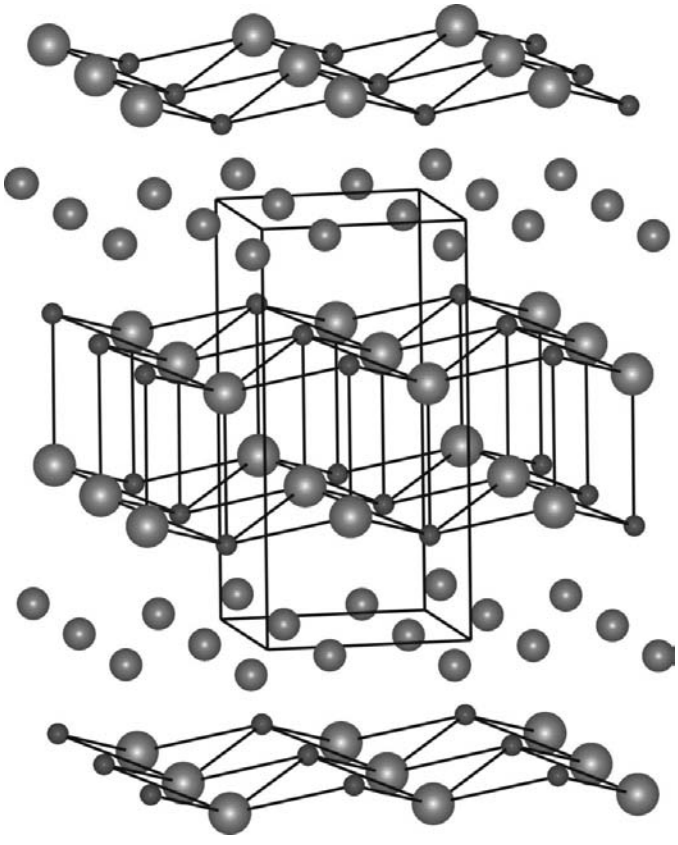

Figure 1
Perspective view of the basic structure of RE polychalcogenides. Small circles correspond to Re atoms, large circles denote X atoms in the ReX layer and circles of intermediate size indicate X atoms in the square layers.

Table 1
Experimental details.

Crystal data	
Chemical formula	$GdS_{1.82}$
Chemical formula weight	215.5
Basic cell setting, space group	Tetragonal, $P4/n$
a, c (Å)	3.8951 (7), 7.9343 (14)
V (Å^3)	120.4 (1)
Z	2
D_x (g cm^{-3})	5.944
D_{meas} (g cm^{-3})	5.88 (8)
Radiation type	Mo $K\alpha$
No. of reflections for cell parameters	24
θ range (°)	60–90
μ (mm^{-1})	28.69
Temperature (K)	293
Crystal form, colour	Ellipsoid, yellowish-orange
Crystal size (mm^3)	0.21 × 0.20 × 0.18
Laue Class	4/m
$\mathbf{q_1}$	[0.252 (4), 0.331 (3), $\frac{1}{2}$]
$\mathbf{q_2}$	[−0.331 (2), 0.252 (4), $\frac{1}{2}$]
Data collection	
Diffractometer	IPDS Stoe
Sample detector distance (mm)	60
Data collection method	Phi oscillation
Absorption correction method	Numerical integration (*HABITUS*)
T_{min}	0.026
T_{max}	0.059
No. of measured, independent and observed reflections	25 287, 3565, 900
Criterion for observed reflections	$I > 3\sigma(I)$
R_{int}	0.064
Range of h, k, l, m_1, m_2	$-5 \le h, k \le 5$ $-12 \le l \le 12$ $-2 \le m_1, m_2 \le 2$
No. of main reflections (all/obs)	990/934
No. of first-order satellites (all/obs)	4164/2307
No. of second-order satellites (all/obs)	5985/703
No. of third-order satellites (all/obs)	6174/37
No. of fourth-order satellites (all/obs)	979/0
No. of unique reflections (all/obs)	3565/900
No. of main reflections (all/obs)	150/145
No. of first-order satellites (all/obs)	573/410
No. of second-order satellites (all/obs)	1148/253
No. of third-order satellites (all/obs)	1136/92
No. of fourth-order satellites (all/obs)	558/0
R_{int}	0.0636
Refinement	
Refinement on	F
$R[F^2 > 2\sigma(F^2)]$, $wR(F^2)$, S	0.040, 0.094, 0.73
No. of reflections	3565
No. of parameters	52
Weighting scheme	Based on measured s.u.'s; $w = 1/[\sigma^2(F) + 0.0025F^2]$
$(\Delta/\sigma)_{max}$	0.002
$\Delta\rho_{max}$, $\Delta\rho_{min}$ (e Å^{-3})	10.55, −11.52
Extinction method	Becker & Coppens (1974)
Extinction coefficient	0.007445

In the revised phase diagram of GdS_{2-x} only the composition $GdS_{1.84(2)}$ has been indicated in the range $0 < x < 0.5$ (Vasilyeva & Kurochkina, 1981; Vasilyeva, 1985). Previously reported compositions such as GdS_2 (Flahaut, 1959), $GsS_{1.7-1.8}$ (Ring & Tecotzky, 1964) and $GdS_{1.9}$ (Loginova, 1974) are either inaccurate or do not correspond to thermodynamically stable phases. Available structural information on GdS_{2-x} is limited to the lattice parameters of the basic structure as

derived from X-ray powder diffraction (Flahaut, 1959; Loginova, 1974; Vasilyeva & Kurochkina, 1981). The peak profiles in Raman spectroscopy, corresponding to the vibrations of the S_2^{2-} dimers, have been found to be different in GdS_{2-x} as opposed to other RE polysulfides (Kolesov & Vasilyeva, 1992). This fact suggests that the distortions in the square layers of GdS_{2-x} might be different from the superstructures observed in $SmS_{1.9}$ (Tamazyan *et al.*, 2000*a*), $DyS_{1.76}$ (Tamazyan *et al.*, 1994) and $HoS_{1.86}$ (Podberezskaya *et al.*, 1999). In this paper we report the crystal structure of $GdS_{1.82}$ as determined from single-crystal X-ray diffraction.

2. Experimental

Crystals of $GdS_{1.82}$ were prepared by spontaneous crystallization, when a melt containing $GdS_{1.84}$ in a KI flux was slowly cooled down from 973 K to room temperature. An equilibrium vapour pressure of sulfur was maintained above the melt. Plate-like crystals with dimensions up to $3 \times 2 \times 1.5$ mm^3 were obtained. The colour varied between yellowish-orange for thin plates and grey with a metallic lustre for thick plates. The largest facets were parallel to the (0 0 1) lattice planes of the basic structure. The density was measured for many individual crystals weighing as much as 4 mg (Table 1).

Several crystals of almost spherical shape ($r \simeq 0.1$ mm) were prepared and glued onto glass fibres for X-ray diffraction experiments. Because of the layered structure it was impossible to prepare perfect spherical samples and the shapes of the crystals were ellipsoidal with the short axes along the [001] directions. The difference between the long and short axes of the ellipsoids varied within 10%. Crystal quality was tested by measuring the profiles of the Bragg reflections in ω scans on an Enraf–Nonius CAD4 diffractometer and a Nonius MACH3 (rotating anode) diffractometer. The best sample with the narrowest reflection profile (full width at half-maximum, FWHM $\simeq 0.15^\circ$) was selected for the diffraction experiment.

The SEARCH procedure on the CAD-4 diffractometer found several strong and a few weak reflections. The strong reflections could be indexed on a tetragonal lattice corresponding to the ZrSSi structure type. The lattice parameters

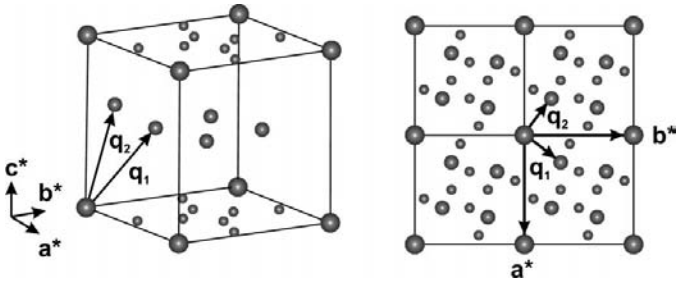

Figure 2
Perspective view and (0 0 1) projection of the diffraction pattern of GdS_{2-x}. The basis vectors $\mathbf{a}^*$, $\mathbf{b}^*$ and $\mathbf{c}^*$ of the reciprocal lattice and the modulation wavevectors $\mathbf{q}_1$ and $\mathbf{q}_2$ are indicated. Large circles correspond to the main reflections; intermediate sized circles denote the first-order satellite reflections; small circles represent second-order satellites.

$a = b = 3.8951\,(1)$ and $c = 7.9343\,(2)$ Å were obtained by refinement of the orientation matrix against the positions of 25 strong reflections with scattering angles in the range $60 < 2\theta < 90^\circ$. Analysis of the fractional indices of the weak reflections showed that they could be indexed with five integer indices $(h\,k\,l\,m_1\,m_2)$ according to

$$\mathbf{H} = h\,\mathbf{a}^* + k\,\mathbf{b}^* + l\,\mathbf{c}^* + m_1\,\mathbf{q}_1 + m_2\,\mathbf{q}_2 \qquad (1)$$

with modulation wavevectors (Fig. 2)

$$\mathbf{q}_1 = \alpha\,\mathbf{a}^* + \beta\,\mathbf{b}^* + \tfrac{1}{2}\,\mathbf{c}^*$$
$$\mathbf{q}_2 = \beta\,\mathbf{a}^* - \alpha\,\mathbf{b}^* + \tfrac{1}{2}\,\mathbf{c}^*. \qquad (2)$$

This shows that the structure can be described as a two-dimensional modulated structure employing the superspace formalism (see below; de Wolff *et al.*, 1981; van Smaalen, 1995).

Previous investigations of RE polysulfides have shown that these compounds exhibit a tendency to form twinned crystals, because of the pseudo-tetragonal lattice (Tamazyan *et al.*, 2000*a*,*b*). A possible twinning in $GdS_{1.82}$ was investigated by analyzing two-dimensional (ω, θ) profiles of selected reflections as they were measured at different azimuthal angles Ψ. Reflection splitting was not observed. Moreover, the ω and θ profiles were practically independent of the crystal orientation. These findings show that the single crystal of GdS_{2-x} used in this study is not twinned. Twinning by merohedry would still be possible if GdS_{2-x} belonged to the Laue class $4/m$. However, in that case additional satellite reflections should have been found with modulation wavevectors $\mathbf{q}_3 = \alpha\,\mathbf{a}^* - \beta\,\mathbf{b}^* + \frac{1}{2}\,\mathbf{c}^*$ and $\mathbf{q}_4 = \beta\,\mathbf{a}^* + \alpha\,\mathbf{b}^* + \frac{1}{2}\,\mathbf{c}^*$ [*cf.* (2)]. The ratios of the intensities of satellite reflections related by twinning operators then give the ratio of the volumes of the twin components. Since satellite reflections with wavevectors $\mathbf{q_3}$ and $\mathbf{q_4}$ have not been observed, we conclude that the sample is not twinned but rather is a true single crystal.

The integrated intensities of the Bragg reflections were measured by a series of image-plate recordings on a Stoe IPDS diffractometer with Mo $K\alpha$ radiation. The integrated intensities of the reflections were obtained with the Stoe software employing the *Q-VECTORS* program. An absorption correction was applied with *HABITUS* (Herrendorf, 1992). Initially the crystal was described as an icosahedron. The refined crystal shape was close to an ellipsoid of revolution with a small difference between the longest and the shortest axes, which closely matches the observed shape.

The components of the modulation wavevectors have rational values within the standard uncertainties of the experiment, with $\alpha = \frac{1}{4}$ and $\beta = \frac{1}{3}$ [(2) and Table 1]. These rational coefficients indicate that the structure can be described on a $12 \times 12 \times 2$ supercell. The supercell is *I*-centred and thus corresponds to a 144-fold superstructure of the ZrSSi structure type. Accordingly, 143 superlattice reflection positions exist for each Bragg reflection of the basic structure. In the superspace description these reflections are described as satellite reflections with $-6 < m_1 \leq 6$ and $-6 < m_2 \leq 6$, where $m_1 = m_2 = 0$ define the main reflections

Table 2
Reflection indices $(m_1\, m_2)$ describing satellites with non-zero intensities [see (1)].

The reflection order is defined as $m = |m_1| + |m_2|$. Reflection orders that do not occur in this table, *e.g.* (20), describe satellites for which zero intensity was observed within the experimental resolution.

Order	$(m_1 m_2)$	Order	$(m_1 m_2)$	Order	$(m_1 m_2)$
1	$\pm(10)$	2	$\pm(\bar{1}1)$	3	$\pm(2\bar{1})$
1	$\pm(01)$	3	$\pm(21)$	3	$\pm(12)$
2	$\pm(11)$	3	$\pm(\bar{1}2)$		

[see (1)]. Inspection of the diffraction data showed that non-zero intensities can only be obtained for 16 combinations $(m_1\, m_2)$ out of a possible 143 (Table 2). This implies that most superlattice reflections have zero intensities. The five-integer indexing systematically describes these absences as high-order satellites (m>3). Consequently, the structure can only be refined with the aid of the superspace method, in which structural parameters need to be included as long as the corresponding orders of satellites have non-zero intensities. Further experimental details are given in Table 1.

3. Refinement of the structure

In the first step the average structure was refined using only the main reflections. The systematic absences were found as $(h\,k\,0)$: $h + k \neq 2n$, but all reflections $(0\,0\,l)$ did have significantly non-zero intensities. This unambiguously determines the space group $P4/n$ for the average structure. This space group is a subgroup of $P4/nmm$, which represents the space group of the undistorted ZrSSi structure type. The positions of the Gd atoms were determined from the Patterson map and the positions of the S atoms were determined from difference-Fourier maps. Refinement of the structure converged to R_F(obs) = 0.0277 [wR_F^2(obs) = 0.0384, R_F(all) = 0.0293 and wR_F^2(all) = 0.0384]. The structural parameters of the average structure from the final refinement are listed in Table 3 and the supplementary material.[1] All refinements were performed with the computer program *JANA*2000 (Petříček & Dušek, 2000).

The modulated structure is described in the superspace formalism (de Wolff *et al.*, 1981; van Smaalen, 1995). Atomic positions are described as the sum of the average positions (Table 2) and the modulation functions. The latter are given as a truncated Fourier series, where the Fourier coefficients are used as independent parameters in the refinement

$$u_i(\bar{x}_{s4}, \bar{x}_{s5}) = \sum_{n_1=0}^{\infty}\sum_{n_2=0}^{\infty} A_i^{n_1,n_2} \cos[2\pi\,(n_1\bar{x}_{s4} + n_2\bar{x}_{s5})] + B_i^{n_1,n_2} \sin[2\pi\,(n_1\bar{x}_{s4} + n_2\bar{x}_{s5})], \quad (3)$$

where $i = 1, 2, 3$ or (x, y, z) and $A_i^{n_1,n_2}$ and $B_i^{n_1,n_2}$ are the structural parameters. The fourth and fifth superspace coordinates are defined by

[1] Supplementary data for this paper are available from the IUCr electronic archives (Reference: CK5000). Services for accessing these data are described at the back of the journal.

Table 3
Selected interatomic distances of the average structure (Å).

Gd—S1 (4×)	2.848 (1)	Gd—S2 (4×)	2.918 (8)
Gd—S1	2.862 (5)	S2—S2 (4×)	2.754 (2)

Table 4
The values R_F(obs) for the final refinements of the incommensurate (Inc) structure model and of the four different commensurate sections of superspace.

Partial R values for different reflection groups are given (see Table 2). The commensurate sections are defined by the space group of the supercell.

Reflections	Inc	$I\bar{4}$	$I4$	$I\bar{1}$	$I1$
All	0.0396	0.0396	0.0396	0.0396	0.0396
$m = 0$	0.0313	0.0313	0.0313	0.0313	0.0313
$m = 1$	0.0332	0.0332	0.0332	0.0332	0.0332
$m = 2$	0.0699	0.0700	0.0699	0.0699	0.0699
$m = 3$	0.1281	0.1272	0.1280	0.1281	0.1281

$$\bar{x}_{s4} = t_1 + \mathbf{q}_1 \cdot \mathbf{r}^0$$
$$\bar{x}_{s5} = t_2 + \mathbf{q}_2 \cdot \mathbf{r}^0, \quad (4)$$

with $\mathbf{r}^0$ denoting the average position of the atoms and (t_1, t_2) defining the section of superspace or the initial phase of the modulation functions. Similar modulation functions were used for the occupation of the S2 site and the temperature factors.

The modulation was initially treated as incommensurate. As many harmonics were introduced as were required to obtain low R values. The displacement modulation of Gd and S2 is described by one harmonic for each group of observed satellites (Table 2). The displacement modulation of S1 and the occupational modulation of S2 are described by a fewer number of harmonics. Furthermore, one harmonic has been used for the modulation of the temperature parameters of Gd. The introduction of higher harmonics led to unstable refinements, while these parameters had large standard uncertainties and values that did not exceed approximately three times their standard uncertainties.

The modulated structure was solved by subsequently introducing the independent modulation parameters with arbitrary but small values. Two (3 + 2)-dimensional superspace groups are compatible with the diffraction symmetry and the average structure, and both of them can occur in two different settings. Given the basic structure positions of the atoms, the four different possibilities for the modulated structures are characterized by superspace groups with the tentative symbols (Janssen *et al.*, 1992): $P4/n(\alpha\beta\frac{1}{2})(00)(00)$,$P4/n(\alpha\beta\frac{1}{2})(00)(s0)$, $P4/n(\alpha\beta\frac{1}{2})(00)(0s)$ and $P4/n(\alpha\beta\frac{1}{2})(00)(ss)$, where the translational components along $(\bar{x}_{s4}\, \bar{x}_{s5})$ refer to the fourfold axis and the glide plane, respectively. Suitable solutions could not be found within $P4/n(\alpha\beta\frac{1}{2})(00)(0s)$ and $P4/n(\alpha\beta\frac{1}{2})(00)(s0)$. The best fit to the diffraction data within the superspace group $P4/n(\alpha\beta\frac{1}{2})(00)(00)$ was obtained for R_F(obs) = 0.0512 with partial R_F(obs) values of $R(m = 0) = 0.0308$, $R(m = 1) = 0.0369$, $R(m = 2) = 0.1058$ and $R(m = 3)$ = 0.3260. The final refinement of the incommensurately modulated structure within the superspace group $P4/n(\alpha\beta\frac{1}{2})(00)(ss)$

Table 5
The symmetry operators of the $(3+2)$-dimensional superspace group $P4/n(\alpha\beta\frac{1}{2})(00)(ss)$ with the origin at the inversion centre.

x_1	x_2	x_3	x_4	x_5
$\frac{1}{2}-x_2$	x_1	x_3	$\frac{1}{2}+x_3-x_5$	$\frac{1}{2}+x_4$
$\frac{1}{2}-x_1$	$\frac{1}{2}-x_2$	x_3	x_3-x_4	x_3-x_5
x_2	$\frac{1}{2}-x_1$	x_3	$\frac{1}{2}+x_5$	$\frac{1}{2}+x_3-x_4$
$-x_1$	$-x_2$	$-x_3$	$-x_4$	$-x_5$
$\frac{1}{2}+x_2$	$-x_1$	$-x_3$	$\frac{1}{2}-x_3+x_5$	$\frac{1}{2}-x_4$
$\frac{1}{2}+x_1$	$\frac{1}{2}+x_2$	$-x_3$	$-x_3+x_4$	$-x_3+x_5$
$-x_2$	$\frac{1}{2}+x_1$	$-x_3$	$\frac{1}{2}-x_5$	$\frac{1}{2}-x_3+x_4$

converged at R_F(obs) = 0.0396 (Table 4). Although the fit to the main reflections is equally good for both symmetries, the latter superspace group gives a much better fit to the satellite reflections, leading to the conclusion that the symmetry of the modulated structure can be described by the superspace group $P4/n(\alpha\beta\frac{1}{2})(00)(ss)$. The symmetry operators are listed in Table 5. The average structure coordinates do not differ from those obtained by the refinement of the average structure (see supplementary material). The modulation amplitudes of the final structure model are given in Table 6.

The observed components of the modulation wavevectors suggest that the modulation is commensurate and that the structure can be described with respect to a $12\times12\times2$ supercell. The supercell is obtained from the superspace model by setting the components of the modulation wavevectors equal to their commensurate values $\alpha=\frac{1}{4}$ and $\beta=\frac{1}{3}$ and by selecting a section of superspace as it is defined by particular values of (t_1, t_2) [see (4)]. Different sections led to different space groups for the supercell (Tamazyan *et al.*, 1996). The sections $[(4n-1)/48,\ (4m-1)/48]$ and $[(4n-3)/48,\ (4m-3)/48]$ correspond to the supercell space group $I4$ (n and m are integers), the sections $[(4n-3)/48,\ (4m-1)/48]$ and $[(4n-1)/48,\ (4m-3)/48]$ correspond to the supercell space group $I\bar{4}$, and the sections $(n/24,\ m/24)$ correspond to the supercell space groups $I\bar{1}$. All other sections correspond to a superstructure with the space group $I1$.

Refinements of the superstructure were performed within the commensurate superspace approach for all four different sections. Within the commensurate refinement the modulation functions are sampled in $12\times12\times2$ equally spaced points in the interval $(0\le t_1<1;\ 0\le t_2<2)$, starting at the values for (t_1, t_2) given in the preceding paragraph. This differs from the incommensurate refinement, which involves an integration over (t_1, t_2). The fit to the data was equally good for all sections (Table 4). They do not allow the true supercell symmetry to be determined. However, the refined modulation amplitudes are independent of the commensurate section (Table 6). The consequences of employing different commensurate sections of superspace are discussed below. It is noted that refinements in the supercell are not possible, because the supercell space group defines a set of crystallographically independent parameters that is a depen-

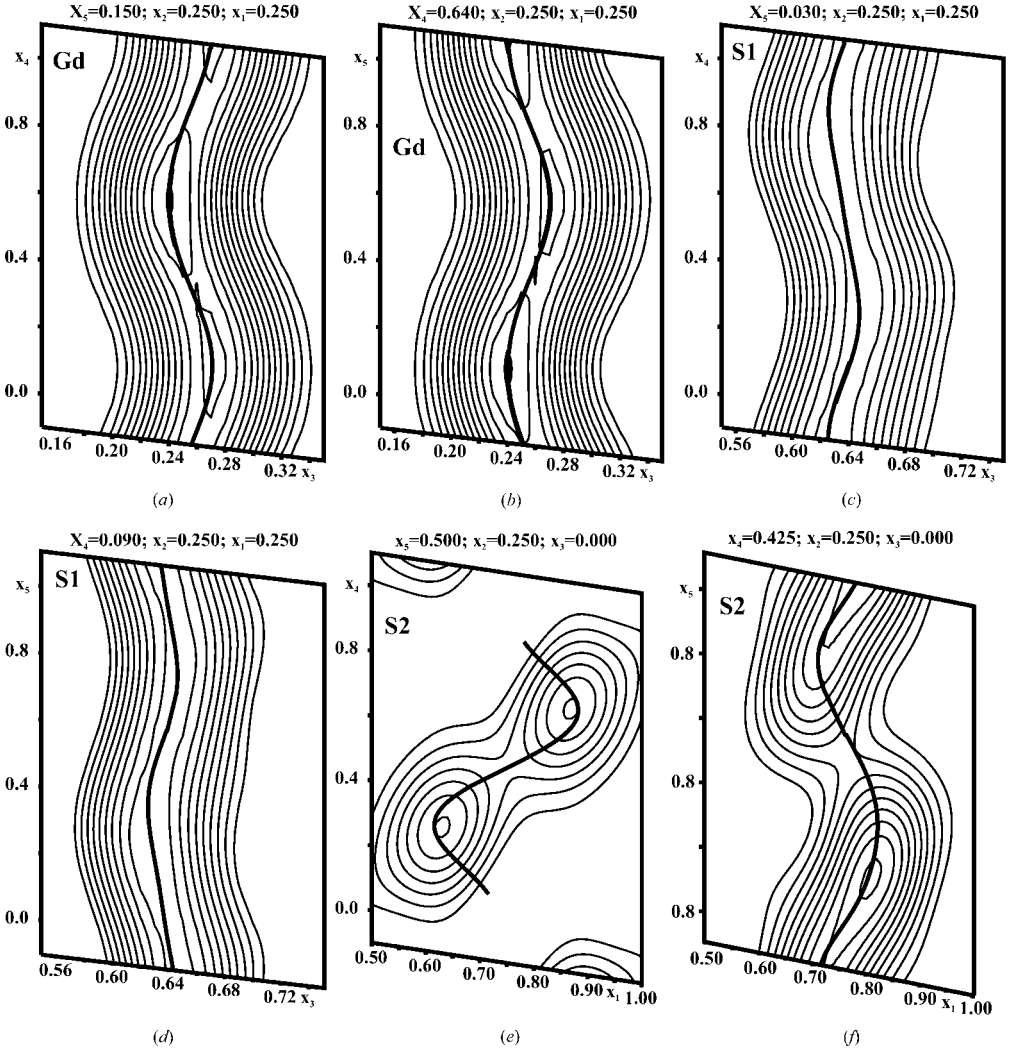

Figure 3
Sections of the Fourier map (F_{obs}). Thin lines refer to contour lines of equal electron density. The modulation functions are displayed by thick lines. The discontinuity of the modulation function of the S2 atom represent the occupational modulation of this atom.

Table 6
Modulation parameters of the final structure model.

Values relative to the lattice of the average structure are given according to (3). Standard uncertainties are given in parentheses. The crystallographically independent parameters are indicated by an asterisk. The value 0 indicates that this parameter is equal to zero, as required by the superspace symmetry.

Atom	$(n_1 n_2)$	$A_x^{n_1,n_2}$	$B_x^{n_1,n_2}$	$A_y^{n_1,n_2}$	$B_y^{n_1,n_2}$	$A_z^{n_1,n_2}$	$B_z^{n_1,n_2}$
Gd	(10)	0.00553 (5)	−0.00477 (5)*	0.00293 (5)	−0.00253 (4)*	0.01215 (3)	0.01409 (4)*
Gd	(01)	0.00293 (5)	−0.00253 (4)	−0.00553 (5)	0.00477 (5)	−0.01215 (3)	−0.01409 (4)
Gd	(11)	−0.00504 (7)	−0.000752 (11)*	0.00244 (8)	0.000364 (11)*	0.000188 (6)	−0.00126 (4)*
Gd	($\bar{1}$1)	0	0.00247 (8)	0	0.00510 (7)	−0.00128 (4)	0
Gd	(2̄1)	0.00293 (5)	0.00464 (8)*	0.00193 (6)	0.00306 (9)*	0.00048 (5)	−0.00030 (3)*
Gd	(1̄2)	0.00274 (8)	−0.00236 (7)	−0.00415 (7)	0.00358 (6)	0.00037 (4)	0.00043 (5)
Gd	(2$\bar{1}$)	−0.00210 (9)	0.00181 (8)*	0.00056 (10)	−0.00048 (8)*	0.00093 (4)	0.00108 (4)*
Gd	(12)	0.00040 (7)	0.00063 (11)	0.00148 (7)	0.00234 (10)	0.00120 (5)	−0.00076 (3)
S1	(10)	−0.0035 (3)	−0.00158 (13)*	−0.0015 (3)	−0.00067 (13)*	−0.00466 (8)	0.01039 (17)*
S1	(01)	−0.0015 (3)	−0.00067 (13)	0.0035 (3)	0.00158 (13)	0.00466 (8)	−0.01039 (17)
S1	(11)	0.0002 (3)	−0.0002 (3)*	0.0009 (3)	−0.0008 (3)*	0.00080 (12)	0.00089 (13)*
S1	($\bar{1}$1)	0	−0.0012 (4)	0	0.0003 (4)	−0.00120 (17)	0
S1	(2̄1)	−0.00132 (15)	−0.0042 (5)*	−0.00104 (16)	−0.0033 (5)*	−0.0007 (3)	0.00023 (9)*
S1	(1̄2)	0.0032 (5)	0.0014 (2)	−0.0040 (4)	−0.0018 (2)	−0.00031 (12)	0.0007 (3)
S2 (Occ)	(10)	−0.269 (5)*	0				
S2 (Occ)	(01)	0.269 (5)	0				
S2 (Occ)	(11)	0.162 (6)*	0				
S2 (Occ)	($\bar{1}$1)	0.162 (6)	0				
S2	(10)	0	−0.0673 (7)*	0	−0.0575 (7)*	−0.0003 (2)*	0
S2	(01)	0	−0.0575 (7)	0	0.0673 (7)	−0.0003 (2)	0
S2	(11)	0	0.0202 (7)*	0	0.0040 (7)*	0.0011 (3)*	0
S2	($\bar{1}$1)	0	−0.0040 (7)	0	0.0202 (7)	−0.0011 (3)	0
S2	(2̄1)	0	−0.0009 (8)*	0	0.0067 (9)*	−0.0006 (4)*	0
S2	(1̄2)	0	0.0067 (9)	0	0.0009 (8)	−0.0006 (4)	0
S2	(2$\bar{1}$)	0	−0.0315 (8)*	0	−0.0129 (8)*	−0.0014 (4)*	0
S2	(12)	0	−0.0129 (8)	0	0.0315 (8)	−0.0014 (4)	0

dent set, as follows from the singular refinement matrix.

4. Discussion

4.1. Incommensurate *versus* commensurate modulations

The quality of the fit to the diffraction data is good, but it does not allow the determination of whether the structure is incommensurately or commensurately modulated, neither can it be used to distinguish the different superstructure models (Table 4). The reason for this feature of the refinements is that many superlattice reflections have zero intensities and that these reflections are classified as satellite reflections of orders $m = 4$ and higher. This makes the commensurate and incommensurate structures similar as far as their diffraction is concerned. The difference between the incommensurate and commensurate structure models is that in the latter the modulation functions are sampled at 144 different points $(\bar{x}_{s4}, \bar{x}_{s5})$. Apparently these points are so dense that the summation with 144 terms and a true integration do not lead to different results. In this respect it should be noted that in refinement programs the integral over the unit cell in superspace is often approximated by a summation over a finite number of points.

Looking at the situation the other way around these observations imply that the continuous modulation functions in the incommensurate structure model give a good approximation to the superstructure. Any point in $(\bar{x}_{s4}, \bar{x}_{s5})$ space is close to a point that is realised in the supercell. It is therefore a

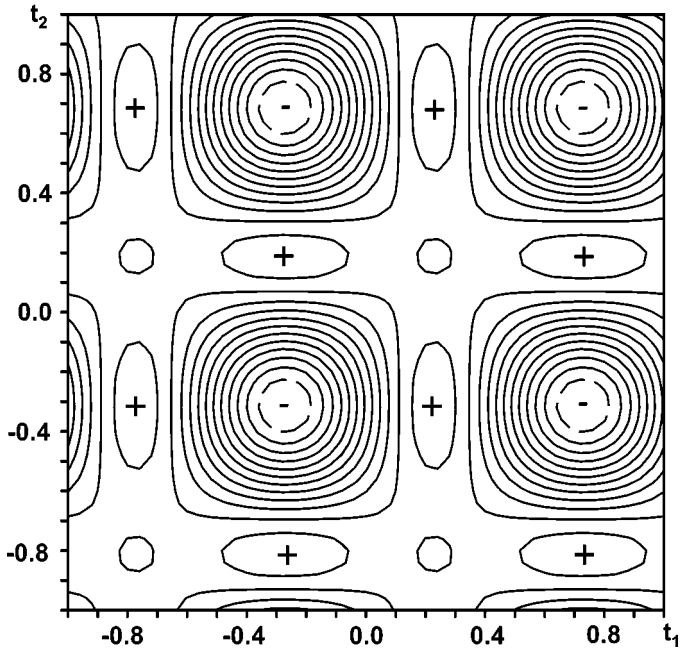

Figure 4
Occupation of the S2 site as a function of (t_1, t_2). The value of the occupation of S2 is given by contour lines according to the structure model in Table 6 and deposited material. Contour lines are at intervals of 0.1. The maximum of 1.16 is marked by + and the minimum of −0.09 is marked by −.

meaningful procedure to analyse the superstructure with the superspace techniques of incommensurate structures, even if the structure is commensurate, as we will do here.

4.2. The modulation functions

Two-dimensional sections of the five-dimensional Fourier map of F_{obs} are given in Fig. 3. They show that the modulations are well described by the refined modulation functions (Table 6). The disconnected character of the maxima centred on the position of the S2 atom reflect the occupational modulation at this site, which appears to vary between 0 and 1. Both the Fourier map (Fig. 3) and the refined modulation function (Fig. 4) indicate that the occupational modulation of S2 might be better described by a two-dimensional block-wave type of function. Unfortunately, such functions, with many more degrees of freedom than simple one-dimensional block waves, are not available in *JANA*2000 or any other computer program. Therefore, we will use the harmonic model as it is presented here. A consequence is that series termination effects lead to occupancies less than zero or larger than one for small regions in (t_1, t_2) space (Fig. 4).

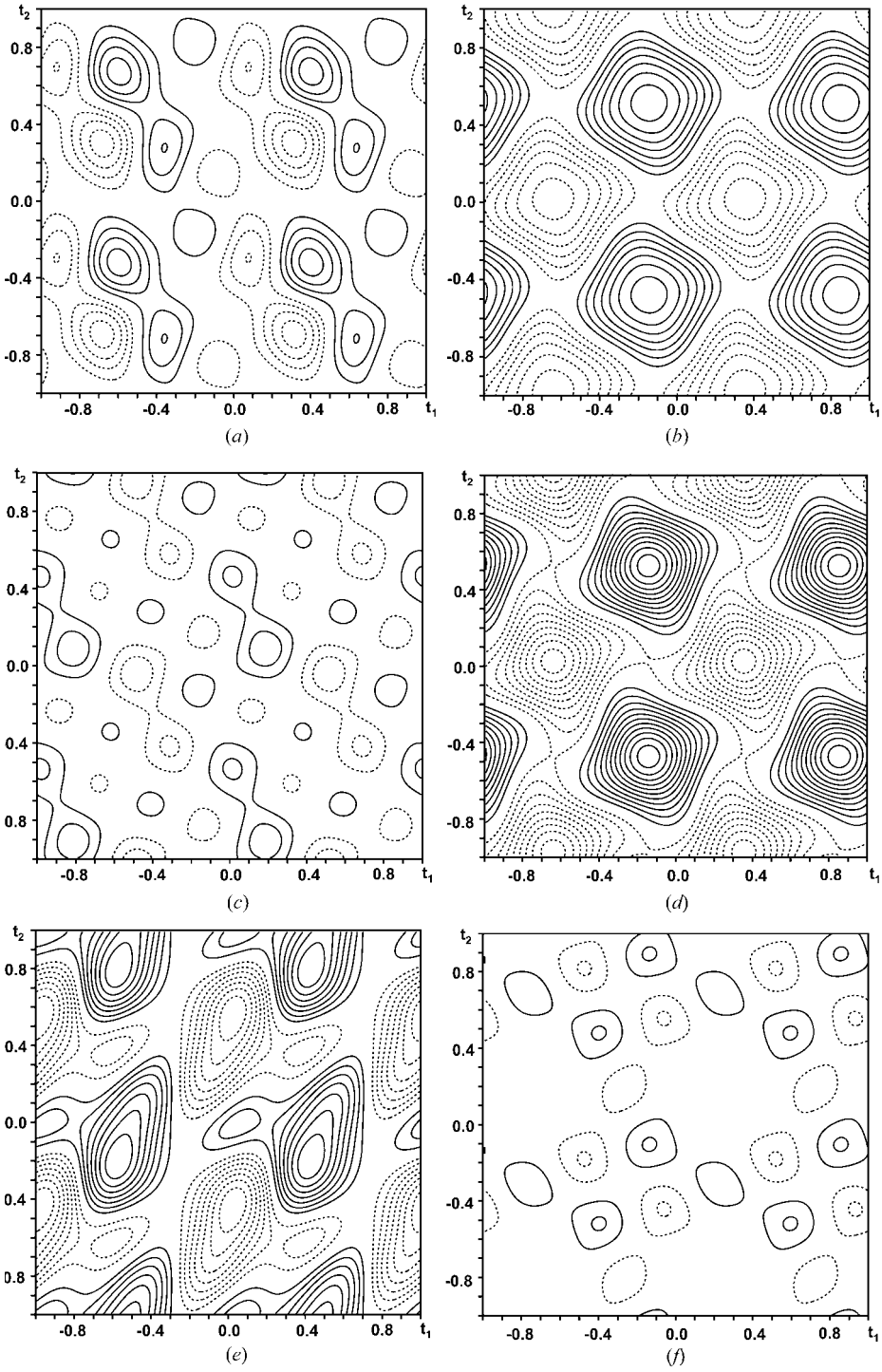

Figure 5
Displacements of the atoms out of their average positions as a function of (t_1, t_2). (*a*) *x* component; (*b*) *z* component of the modulation of Gd; (*c*) *x* component; (*d*) *z* component of the modulation of S1; (*e*) *x* component; (*f*) *z* component of the modulation of S2. Shown are contours of equal displacements. Full lines indicate displacements into the positive directions and broken lines indicate displacements into the negative directions. Contour lines are at intervals of 0.02 Å in (*a*), (*c*), (*d*) and (*f*), at intervals of 0.04 Å in (*b*) and at intervals of 0.08 Å in (*e*).

4.3. Correlated displacements

The fact that fully occupied and empty S2 sites are found for the structure model refined with only a few harmonics strongly suggests that the superstructure of $GdS_{1.82}$ corresponds to an ordering of vacancies in the planes of the S2 atoms. The largest displacement modulation is found for the displacements of the S2 atoms parallel to the square planes (**ab** plane). The displacement along **c** is almost zero (Fig. 5). These observations suggest that the displacements of S2 are responsible for the formation of S_2^{2-} and S^{2-} ions, as is shown to be true below.

Correlations between the displacement modulations of neighbouring atoms, and between displacement modulations and the vacancy ordering on the S2 site can be analysed by *t* plots of the modulation functions themselves (Figs. 4 and 5), *t* plots of the interatomic distances and *t* plots of the valences of the atoms. For the Gd atom the neighbouring atoms to be considered are the five S1 atoms and the four S2 atoms in its first

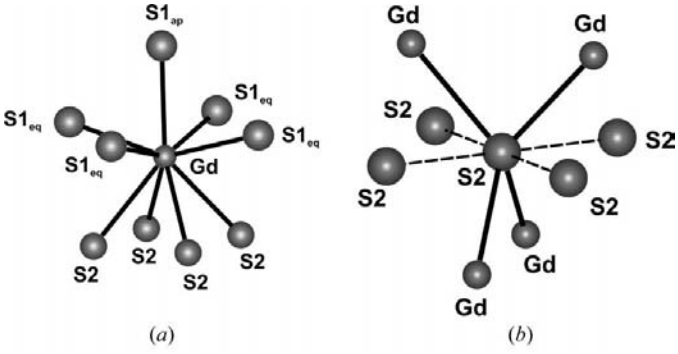

Figure 6
Coordination of (*a*) Gd and (*b*) S2 atoms. The Gd—S bonds are indicated by full lines, while possible S—S bonds are indicated by broken lines.

coordination sphere. The S1 atoms form a square pyramid with four equatorial $S1_{eq}$ atoms at equal distances and one apical $S1_{ap}$ atom. Four S2 atoms at equal distances are arranged opposite to the square face of the pyramid (Table 3 and Fig. 6*a*). The first coordination sphere of S2 contains four Gd atoms at equal distances in a tetrahedral coordination and four S2 atoms (S2 sites) at equal distances within the same plane (Fig. 6*b*). In the modulated structure each of these distances becomes a function of (t_1, t_2), resulting in the observed variations of distances in the *t* plots (Fig. 7). Their average, minimum and maximum values are given in Table 7.

Valences of the atoms have been computed as a function of (t_1, t_2) by the bond-valence method (Brown, 1992; Brese & O'Keeffe, 1991; O'Keeffe & Brese, 1992; van Smaalen, 1995). The atoms in the first coordination spheres, as they are defined above, were incorporated into the calculation (Fig. 6). Bond-valence parameters were taken from Brese & O'Keeffe (1991) and O'Keeffe & Brese (1992). Both the valences of the atoms and the partial contributions towards the valences of the Gd atoms only, the S1 atoms only or the S2 atoms only have been computed (Fig. 8). Contributions of the S2 atoms were weighted according to the fractional occupancy of this site.

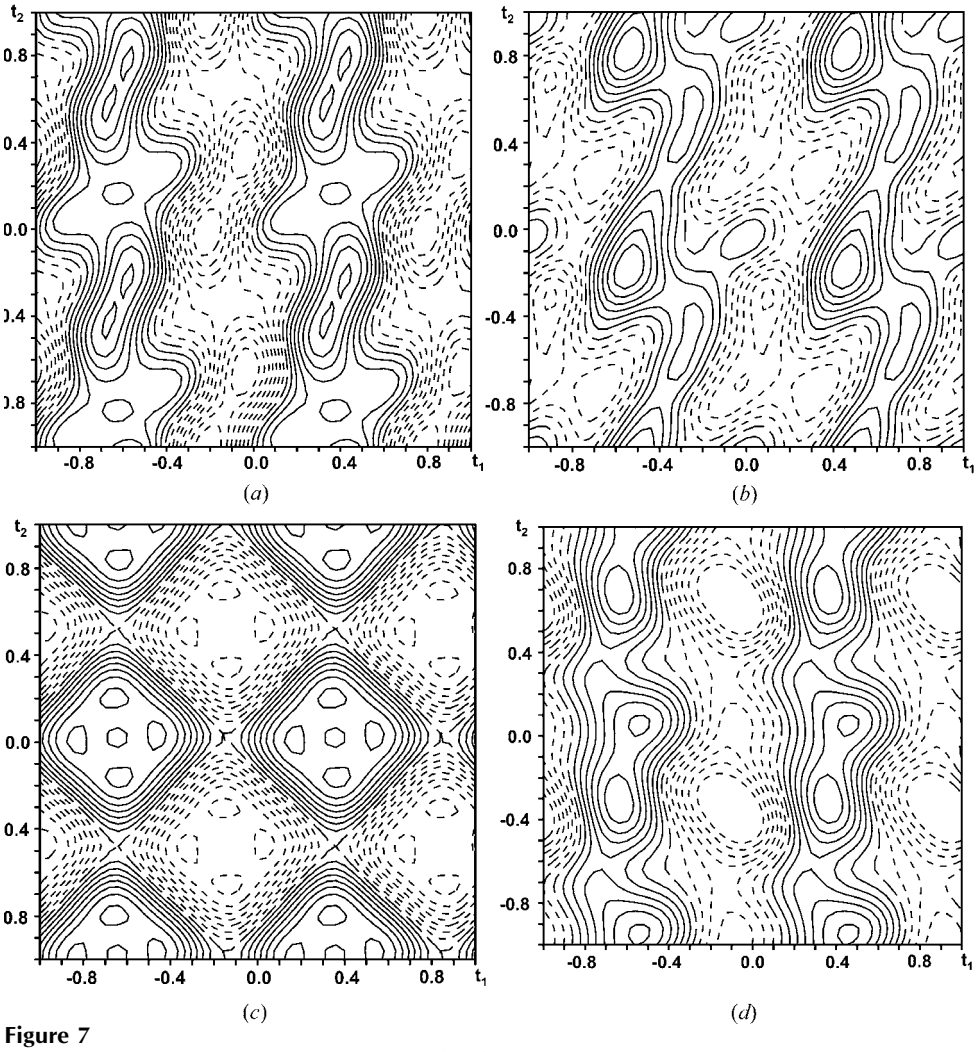

Figure 7
Selected interatomic distances as a function of (t_1, t_2). Positive contours (full lines) indicate distances larger than average and negative contours (broken lines) indicate distances shorter than average. (*a*) S2—S2 distance between the S2 atoms at $(\frac{3}{4}, \frac{1}{4}, 0)$ and S2 at $(\frac{1}{4}, -\frac{1}{4}, 0)$ (see deposited material). The average distance is 2.754 Å; the contour lines are at intervals of 0.1 Å. (*b*) Gd—S2 distance between the Gd atoms at $(\frac{1}{4}, \frac{1}{4}, 0.2739)$ and S2 at $(\frac{3}{4}, \frac{1}{4}, 0)$. The average distance is 2.942 Å; the contour lines are at intervals of 0.05 Å. (*c*) Gd—$S1_{ap}$ distance (see Fig. 6) between the Gd atoms at $(\frac{1}{4}, \frac{1}{4}, 0.2739)$ and S1 at $(\frac{1}{4}, \frac{1}{4}, 0.6341)$. The average distance is 2.861 Å; the contour lines are at an intervals of 0.01 Å. (*d*) Gd—$S1_{eq}$ distance between the Gd atoms at $(\frac{1}{4}, \frac{1}{4}, 0.2739)$ and S1 at $(-\frac{1}{4}, -\frac{1}{4}, 0.3659)$. The average distance is 2.854 Å; contour lines are at intervals of 0.01 Å.

The major parts of the modulation of Gd and S1 are displacements along **c** (Fig. 5 and Table 6). These displacements are found to be in-phase, implying that the modulation of the GdS slabs can be interpreted as leading to a corrugation of these slabs. Inspection of the *t* plots of the distances makes clear that the nearest-neighbour Gd—S1 distances vary within a narrow range, confirming the coherence between the modulations of these two atoms (Fig. 7). Comparison of the *t* plots shows that shifts of Gd and S1 are directed towards the neighbouring square plane of S2 in the case of the fully occupied S2 sites and away from the square layer if the S2 sites are vacant. This indicates that the vacancy ordering is the driving force for the modulation, while the displacement modulation adapts itself to the occupational modulation in order to keep a suffi-

cient number of strong chemical bonds (short contacts, but not too short) between Gd and S2.

Disregarding the occupational modulation, the largest variation of nearest-neighbour distances occurs for the S2—S2 contact (Table 3 and Fig. 7*a*). Distances are found that are considerably shorter than the expected bond length of an S_2^{2-} dimer of ∼2.2 Å. Since these short distances occur between partially occupied sites, one of them will actually be a vacancy, thus removing these physically meaningless short distances. An S_2^{2-} dimer contains a full S—S bond, *i.e.* each sulfur gives a contribution of 1 to the valence of the other S atom in the dimer. With the formal number of $(S2)^{2-}$ dimers, S^{2-} ions and vacancies as given by the chemical formula (§1), the average number of S—S bonds for each S2 site computes as $(1 - 2x) = 0.64$. The observed average contribution of S2—S2 contacts to the valence of S2 is in good agreement with this ideal value (Table 8). The observed variation of this contribution to the valence is from −0.11 to 1.64. These physically meaningless extreme values will be due to the imperfections of the structure model, as was introduced by the harmonic functions describing a two-dimensional block-wave type of function for the occupational modulation of S2 (Fig. 8*b* and §4.2). Despite these imperfections, the observed values indicate the presence

Table 7
Selected interatomic distances (Å).

First site	Second site	Average	Minimum	Maximum
Gd	S1	2.862 (12)	2.774 (12)	2.948 (12)
Gd	S1	2.852 (11)	2.752 (10)	2.937 (11)
Gd	S1	2.856 (11)	2.752 (10)	2.937 (12)
Gd	S1	2.856 (11)	2.752 (10)	2.937 (10)
Gd	S1	2.853 (11)	2.752 (11)	2.938 (11)
Gd	S2	2.943 (19)	2.722 (17)	3.234 (19)
Gd	S2	2.938 (19)	2.723 (17)	3.235 (19)
Gd	S2	2.942 (19)	2.727 (17)	3.234 (18)
Gd	S2	2.937 (19)	2.724 (17)	3.231 (18)
S2	S2	2.76 (3)	1.87 (3)	3.55 (3)
S2	S2	2.81 (3)	1.86 (3)	3.55 (3)
S2	S2	2.77 (3)	1.87 (3)	3.55 (3)
S2	S2	2.80 (3)	1.87 (3)	3.55 (3)

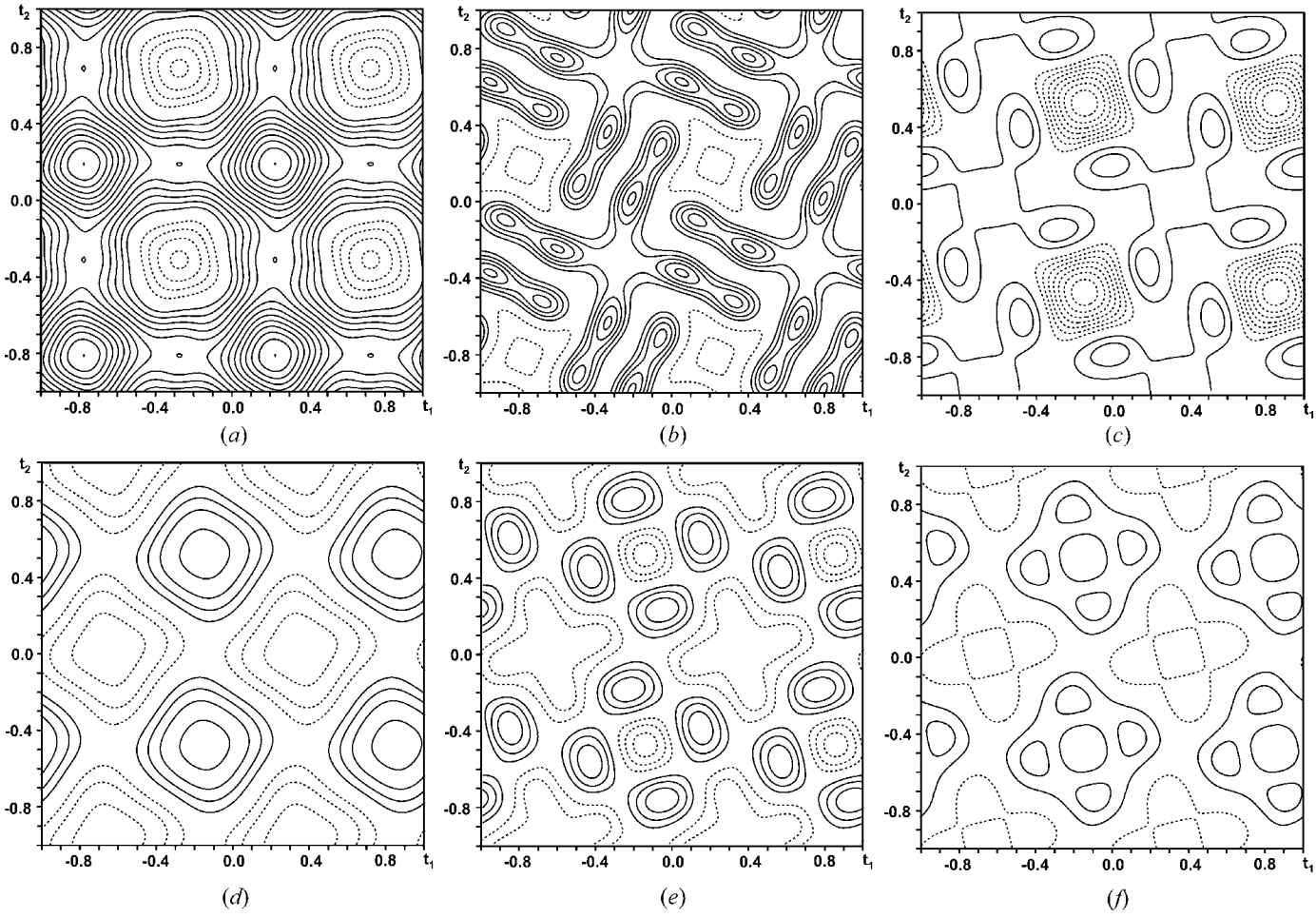

Figure 8
Atomic valences computed by the bond-valence method as a function of (t_1, t_2). The positive (full lines) and negative contours (broken lines) indicate valence contributions which are larger and smaller, respectively, than the average valence contributions given in Table 8. Bond-valence parameters are R_0(Gd—S) = 2.53 and R_0(S—S) = 2.06 Å (Brese & O'Keeffe, 1991; O'Keeffe & Brese, 1992). (*a*) Contribution of the Gd atoms to the valence of S2. (*b*) Contribution of the S2 atoms to the valence of S2. (*c*) Contribution of the S2 atoms to the valence of Gd. (*d*) Contribution of the S1 atoms to the valence of Gd. (*e*) The valence of Gd obtained as the sum of the contributions of S1 and S2 atoms. (*f*) The valence of S1 obtained by the contributions of the five Gd atoms in its first coordination shell. The contour lines are at intervals of 0.05 in (*a*) and (*f*), at intervals of 0.1 in (*c*), (*d*) and (*e*), and at intervals of 0.2 in (*b*).

Table 8
Valences of the atoms Gd and S2 as obtained with the bond-valence method.

Valences of the atoms Gd and S2 as obtained with the bond-valence method.

Atom	Contribution from	Average	Minimum	Maximum
Gd	S1	2.09	1.74	2.52
Gd	S2	1.17	0.40	1.43
Gd	All atoms	3.27	2.91	3.66
S1	Gd	2.09	2.00	2.21
S2	Gd	1.17	0.98	1.88
S2	S2	0.70	−0.11	1.64
S2	All atoms	1.87	1.84	3.09

of S_2^{2-} dimers and S^{2-} ions. The observed average contribution of Gd to the valence of S2 is slightly larger than the expected value of 1 (Table 8). Again, the origin for this discrepancy will lie in the imperfect description of the occupational modulation of S2. As can be seen by comparing the t plots of all eight atoms coordinating S2, the variations of the bond valences compensate each other to a large extent (Fig. 8). These features are in agreement with the displacement modulation of Gd being induced by the vacancy ordering in the S2 layers. The observation that the displacements of S2 along [001] are very small supports the interpretation that the origin for the modulation is a vacancy ordering within the square layers.

The average contribution of S2 to the valence of Gd is equal to the average contribution of Gd to the valence of S2, but the variations are not equal and they are smaller for the former valence (Table 8). The variation of the valence of Gd because of S2 is partially compensated by variations of the contributions of S1 to this valence (Fig. 8*d*). The remaining variations of the valence of Gd will again be because of imperfections in the structure model for the S2 atoms. This conclusion is supported by Figs. 8(*b*) and (*e*), which show that the highest values of the valence of Gd are caused by contributions of the S2 atoms. The valence of S1 (contributions of only Gd) varies much less than the contribution of S1 to the valence of Gd, although the average valence of S1 is again close to the expected value of 2 (Figs. 8*d* and *f*). Similar features of Gd—S1 bonds have also been observed for $DyS_{1.76}$ and $SmS_{1.9}$ (Tamazyan *et al.*, 1994, 2000*a*).

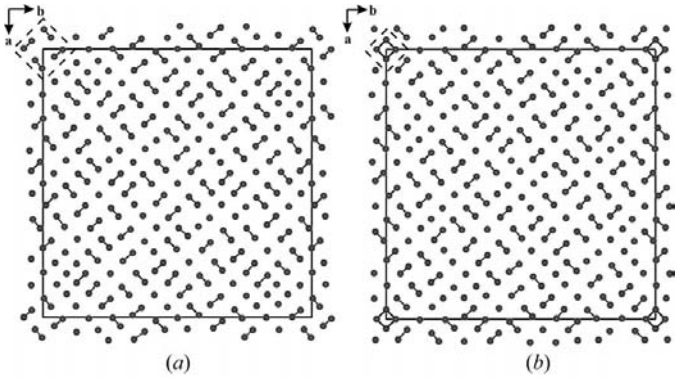

Figure 9
The square layers of S atoms for two commensurate sections of superspace. One unit cell of the $12 \times 12 \times 2$ superstructure is shown for (*a*) supercell space group $I\bar{4}$ and (*b*) supercell space group $I4$. The positions with occupancy lower than 0.1 are considered as vacant positions. S atoms participating in S_2^{2-} dimers are connected by lines. The S_2^{2-} dimers are recognized owing to S—S bond lengths and bond-valence calculations.

4.4. The superstructure

The observed values of the components of the modulation wavevectors indicate that the modulation is commensurate and that it can be described as an ordinary three-dimensional superstructure with a $12 \times 12 \times 2$ I-centred supercell (§3). The refinements are in agreement with this conclusion, but they cannot distinguish between the incommensurate model and various commensurate structure models (Table 4). Fortunately, the modulation amplitudes have equal values for all models and the different superstructures can be obtained from the modulated structure model by computing the appropriate section of superspace, *i.e.* by computing the atomic positions and occupations for the appropriate values of $(\bar{x}_{s4}, \bar{x}_{s5})$. The absence of splitting of the Bragg reflections indicates that there is no evidence for a lattice symmetry lower than tetragonal. Therefore, two sections of superspace remain as possible symmetries of the superstructure, with space groups $I\bar{4}$ and $I4$, respectively.

The structures of the square layers are plotted in Fig. 9. For both model vacancies, S_2^{2-} dimers and isolated S^{2-} ions are observed. As described in §4.3, very small values are found for part of the supposed S_2^{2-} dimers (1.87 Å, see Table 7) and one of the two sites involved will be a vacancy. The analysis of the fractional occupancies of the S2 sites shows that the sum of the occupancies of the two sites, constituting a S_2^{2-} dimer with too short a distance, is always less than 1 for the $I\bar{4}$ superstructure, while it can be larger than 1 for the $I4$ model. Furthermore, the $I4$ model exhibits the formation of square S_4^0 complex ions (Fig. 9). Such a polyanion has never been observed for RE polysulfides and it is highly unlikely to be stable. The $I\bar{4}$ superstructure does not contain this unlikely structural feature. The ring formed from four dimers around a vacancy (Fig. 4) is a local structural feature that has also been observed in other RE polychalcogenides.

Taken together, the observed structural features strongly suggest that the true superstructure is given by the model with $I\bar{4}$ symmetry.

When $x = 0.18$ a fraction of the S2 sites in the square layers are vacancies, as has been determined by the refinement of the average structure. This value is close to the fractional number 13/72. The 144-fold superstructure then contains 2×72 unit cells of the basic structure. The concentration of vacancies is thus in agreement with a complete ordering of vacancies on the square layers, resulting in the observed superlattice. Again, this is a weak argument in favour of a commensurate superstructure as opposed to an incommensurate modulation. It should be noted that similar correlations between composition and order of superstructures were observed for $SmS_{1.9}$ (10-fold superstructure) and $DyS_{1.76}$ (24-fold superstructure).

5. Conclusions

The main results of the present investigations may be summarized as follows:

(i) The 144-fold superstructure of $GdS_{1.82}$ can be described as a two-dimensional modulated structure with a symmetry given by the $(3+2)$-dimensional superspace group $P4/n(\alpha\beta\frac{1}{2})(00)(ss)$. The superspace model allows restrictions on the structural parameters that reach beyond those of the space group of the supercell, *i.e.* all harmonics larger than $n = 3$ have been set equal to zero.

(ii) The incommensurately modulated structure and all the various commensurate superstructure models give equally good fits to the diffraction data.

(iii) Within experimental accuracy the components of the modulation wavevectors are equal to rational values $\alpha = \frac{1}{4}$ and $\beta = \frac{1}{3}$. Accordingly the structure can be described on a $12 \times 12 \times 2$ I-centred supercell. Arguments of structural plausibility indicate that the superstructure has the space group $I\bar{4}$, corresponding to a section of superspace given by (t_1, t_2) equal to $[(4n-1)/48,\ (4m-3)/48]$ or $[(4n-3)/48,\ (4m-1)/48]$ (n and m are integers).

(iv) The fact that the concentration of vacancies $x = 0.18$ is close to the commensurate value 13/72 is in agreement with the complete vacancy order on the observed 144-fold supercell, suggesting that the modulation is indeed commensurate.

(v) The ordering of vacancies and the orientational ordering of S_2^{2-} dimers in the square layers of the S atoms has been identified as the driving force for the structural modulation.

Dr. Wolfgang Millius is thanked for his assistance with the experiment on the Stoe IPDS diffractometer. The German Science Foundation (DFG) and Armenian National Foundation of Science and Advanced Technologies (NFSAT) are gratefully acknowledged for financial support.

References

Becker, P. & Coppens, P. (1974). *Acta Cryst.* A**30**, 129–147.

Böttcher, P. (1988). *Angew. Chem.* **100**, 781–794.

Böttcher, P. & Doert, T. (1998). *Phosphorus Sulfur Silicon*, **137/138**, 255–282.

Böttcher, P., Doert, T., Arnold, H. & Tamazyan, R. (2000). *Z. Kristallogr.* **215**, 246–253.

Brese, N. & O'Keeffe, M. (1991). *Acta Cryst.* B**47**, 192–197.

Brown, I. D. (1992). *Acta Cryst.* B**48**, 553–572.

Dashjav, E., Doert, T., Böttcher, P., Oeckler, O. & Mattausch, H. (2000). *Z. Kristallogr.* **215**, 337–338.

Dashjav, E., Oeckler, O., Doert, T., Mattausch, H. & Böttcher, P. (2000). *Angew. Chem.* **112**, 2089–2090.

Flahaut, H. (1959). *Bull. Chem. Soc.* **10/12**, 1917.

Fokwa, B. P. T., Doert, T. & Böttcher, P. (2002). *Z. Anorg. Allg. Chem.* **628**, 2168.

Fokwa, B. P. T., Doert, T., Simon, P., Söhnel, T. & Böttcher, P. (2002*a*). *Z. Anorg. Allg. Chem.* **628**, 2612.

Fokwa, B. P. T., Doert, T., Simon, P., Söhnel, T. & Böttcher, P. (2002*b*). *Z. Anorg. Allg. Chem.* **628**, 2147.

Herrendorf, W. (1992). PhD thesis. University of Karlsruhe, Germany.

Janssen, T., Janner, A., Looijenga-Vos, A. & De Wolff, P. M. (1992). *International Tables for Crystallography*, Vol. C, edited by A. J. C. Wilson, p. 797. Dordrecht: Kluwer Academic Publishers.

Kolesov, B. & Vasilyeva, I. (1992). *Mater. Res. Bull.* **27**, 775–781.

Lee, S. & Foran, B. (1994). *J. Am. Chem. Soc.* **116**, 154–161.

Lee, S. & Foran, B. (1996). *J. Am. Chem. Soc.* **118**, 9139–9147.

Loginova, E. M. (1974). PhD thesis. Institute of Rare Earth Industry, Moscow.

O'Keeffe, M. & Brese, N. (1992). *Acta Cryst.* B**48**, 152–154.

Petříček, V. & Dušek, M. (2000). *JANA*2000. Institute of Physics of the Academy of Sciences, Praha, Czech Republic.

Podberezskaya, N., Naumov, D., Pervuchina, N., Vasilyeva, I., Magaril, S. & Borisov, S. (1998). *Zh. Struct. Khimii (Russ.)* **39**, 872–874.

Podberezskaya, N., Pervuchina, N., Belaya, S., Vasilyeva, I. & Borisov, S. (2001). *Zh. Struct. Khimii (Russ.)* **42**, 741–752.

Podberezskaya, N., Pervuchina, N., Vasilyeva, I., Magaril, S. & Borisov, S. (1999). *Zh. Struct. Khimii (Russ.)* **40**, 520–529.

Ring, S. & Tecotzky, M. (1964). *Inorg. Chem.* **3**, 182–185.

Smaalen, S. van (1995). *Crystallogr. Rev.* **4**, 79–202.

Stöwe, K. (2000). *J. Solid State Chem.* **149**, 155–166.

Tamazyan, R., Arnold, H., Molchanov, V., Kuzmicheva, G. & Vasilyeva, I. (2000*a*). *Z. Kristallogr.* **215**, 346–351.

Tamazyan, R., Arnold, H., Molchanov, V., Kuzmicheva, G. & Vasilyeva, I. (2000*b*). *Z. Kristallogr.* **215**, 272–277.

Tamazyan, R., Arnold, H. & Petricek, V. (1996). *The Problems of Modern Crystallography, Structural Investigations of Crystals, Transformation of Four-Dimensional Superspace Groups into Three-Dimensional Space Groups for the Commensurately Modulated Structures*, p. 446. Nauka Fizmatlit (in Russian).

Tamazyan, R., Molchanov, V., Kuzmicheva, G. & Vasilyeva, I. (1994). *Zh. Neorg. Khimii (Russ.)* **39**, 417–423.

Vasilyeva, I. (1985). *Izv. Acad. Nauk SSSR, Ser. Neorg. Mater. (Russ.)* **21**, 1043–1045.

Vasilyeva, I. & Kurochkina, L. (1981). *Zh. Neorg. Khimii (Russ.)* **26**, 1872–1876.

Villars, P. & Calvert, L. D. (1996). *Pearson's Handbook of Crystallographic Data for Intermetallic Phases*, 2nd Ed. Materials Park, Ohio: The Materials Information Society.

Wolff, P. M. de, Janssen, T. & Janner, A. (1981). *Acta Cryst.* A**37**, 625–636.

Wu, Y., Doert, T. & Böttcher, P. (2002*a*). *Z. Anorg. Allg. Chem.* **628**, 2216.

Wu, Y., Doert, T., Böttcher, P. & Wu, H. (2002*b*). *Z. Anorg. Allg. Chem.* **628**, 2215.